TABLE 5 Comparison of genetic distances among core subgroups related to aa 70 residues

Patient(s)[a]	Genetic distance (mean ± SD) between two core sequences[b]			Comparison of genetic distance measurements					
				Non-R–R vs non-R–non-R		Non-R–R vs R-R		Non-R–non-R vs R-R	
	Non-R–non-R	Non-R–R	R-R	Larger genetic distance	*P*	Larger genetic distance	*P*	Larger genetic distance	*P*
All ($n = 79$)	0.0349 ± 0.0101	0.0379 ± 0.0109	0.0401 ± 0.0113	Non-R–R	<0.001	R-R	<0.001	R-R	<0.001
CH									
Pt 1	0.0086 ± 0.0042	0.0098 ± 0.0037	0.0064 ± 0.0042	Non-R–R	<0.001	Non-R–R	<0.001	Non-R–non-R	<0.001
Pt 2	0.0097 ± 0.0048	0.0104 ± 0.0041	0.0087 ± 0.0038	Non-R–R	<0.001	Non-R–R	<0.001	Non-R–non-R	0.009
Pt 3	0.0107 ± 0.0058	0.0137 ± 0.0050	0.0034 ± 0.0022	Non-R–R	<0.001	Non-R–R	<0.001	Non-R–non-R	<0.001
LC									
Pt 4	0.0078 ± 0.0036	0.0103 ± 0.0038	0.0053 ± 0.0029	Non-R–R	<0.001	Non-R–R	<0.001	Non-R–non-R	<0.001
Pt 5	0.0118 ± 0.0090	0.0232 ± 0.0085	0.0159 ± 0.0170	Non-R–R	<0.001	Non-R–R	<0.001	No difference	0.991
Pt 6	0.0115 ± 0.0057	0.0121 ± 0.0055	0.0108 ± 0.0056	Non-R–R	<0.001	Non-R–R	<0.001	Non-R–non-R	<0.001
Pt 7	0.0141 ± 0.0085	0.0146 ± 0.0070	0.0136 ± 0.0067	Non-R–R	0.002	Non-R–R	<0.001	Non-R–non-R	<0.001
HCC									
Pt 8	0.0124 ± 0.0063	0.0225 ± 0.0060	0.0181 ± 0.0094	Non-R–R	<0.001	Non-R–R	<0.001	R-R	<0.001
Pt 9	0.0082 ± 0.0042	0.0162 ± 0.0047	0.0078 ± 0.0050	Non-R–R	<0.001	Non-R–R	<0.001	Non-R–non-R	<0.001

[a] Pt, patient.

[b] Non-R–non-R, comparison of two core sequences with residues other than R at aa 70; Non-R–R, comparison of a core sequence with a residue other than R at aa 70 and a core sequence with aa 70R; R-R, comparison of two core sequences with aa 70R. Genetic distances were calculated for all patients by using dominant sequences and for a single patient by using quasispecies sequences.

core sequence with aa 70R and a core sequence with aa 70non-R (non-R–R), demonstrating that core sequences with aa 70R were heterogeneous, while core sequences with aa 70non-R were homogeneous.

Next, to determine the association of the remainder of the core sequences in a single patient, phylogenetic trees were also constructed for each of the nine patients with high mixture rates (5% or more) of R and non-R residues at core aa 70 (Fig. 3B). As shown in Fig. 3B, HCV isolates with core aa 70R and those with core aa 70non-R formed distinctly clustered subgroups on the phylogenetic tree, according to the mutation status at core aa 70. Comparison of genetic distances also proved the finding that HCV isolates with core aa 70R and those with core aa 70non-R form distinctly clustered subgroups on the phylogenetic tree in a single patient, since genetic distances calculated between every two core sequences with aa 70R (R-R) or between every two core sequences with aa 70non-R (non-R–non-R) were significantly smaller than those between a core sequence with aa 70R and a core sequence with aa 70non-R (non-R–R). On the other hand, no significant difference was found when the genetic distance between two core sequences with aa 70non-R (non-R–non-R) and that between two core sequences with aa 70R (R-R) were compared in a single patient (Table 5).

Since the genetic relationships of the remainder of the core sequences were found to differ significantly according to the core aa 70 residue, we then investigated whether there are any common haplotypic sequences specific to each residue. In the comparison of dominant sequences in all 79 patients, most amino acid substitutions clustered in three amino acids (aa 70, aa 75, and aa 91) both in core sequences with aa 70R and in those with aa 70nonR, but no other substitutions specific to each core aa 70 residue were found (Fig. 4).

Quasispecies at core aa 70 and clinical characteristics. To clarify the association of the core aa 70 quasispecies with the clinical picture, levels of gamma-glutamyl transpeptidase (γ-GTP), albumin, platelets, and alpha-fetoprotein, as well as disease progression in the liver, were investigated for correlation with the core aa 70R/non-R mixture ratio. As shown in Fig. 5A and B, the values for these clinical parameters became significantly more abnormal as the proportion of non-R residues increased, showing that a high proportion of non-R residues at core aa 70 was significantly associated with disease severity and hepatocarcinogenesis.

DISCUSSION

This study examined, for the first time, the relationship between the progression of liver disease and the quasispecies nature of the HCV core region (already known to be associated with liver disease progression) by deep sequencing, with the focus on the core aa 70 residue. The analysis revealed that core aa 70 existed as a mixture of "mutant" Q/H (non-R) and "wild-type" R residues in most of the patients and that the proportion of mutant residues increased as liver disease advanced to LC and HCC. Meanwhile, phylogenetic analysis showed that the viral sequences of the almost-entire core region differed genetically depending on the status of core aa 70.

Before starting the analysis, we verified the rate of background error associated with the process of pyrosequencing by analyzing the control plasmid pCV-J4L6S (Fig. 1). Homopolymers of repeated bases, a weak point of pyrosequencing, were generated at two sites, with the same base appearing five and six times. The overall mutation rate at other sites was 0.092% ± 0.005%, and a mutation rate of 0.102% (mean + 2 SDs) or higher was defined as significant in the analysis, in order to avoid detecting background errors.

We focused our analysis on the quasispecies state of core aa 70,

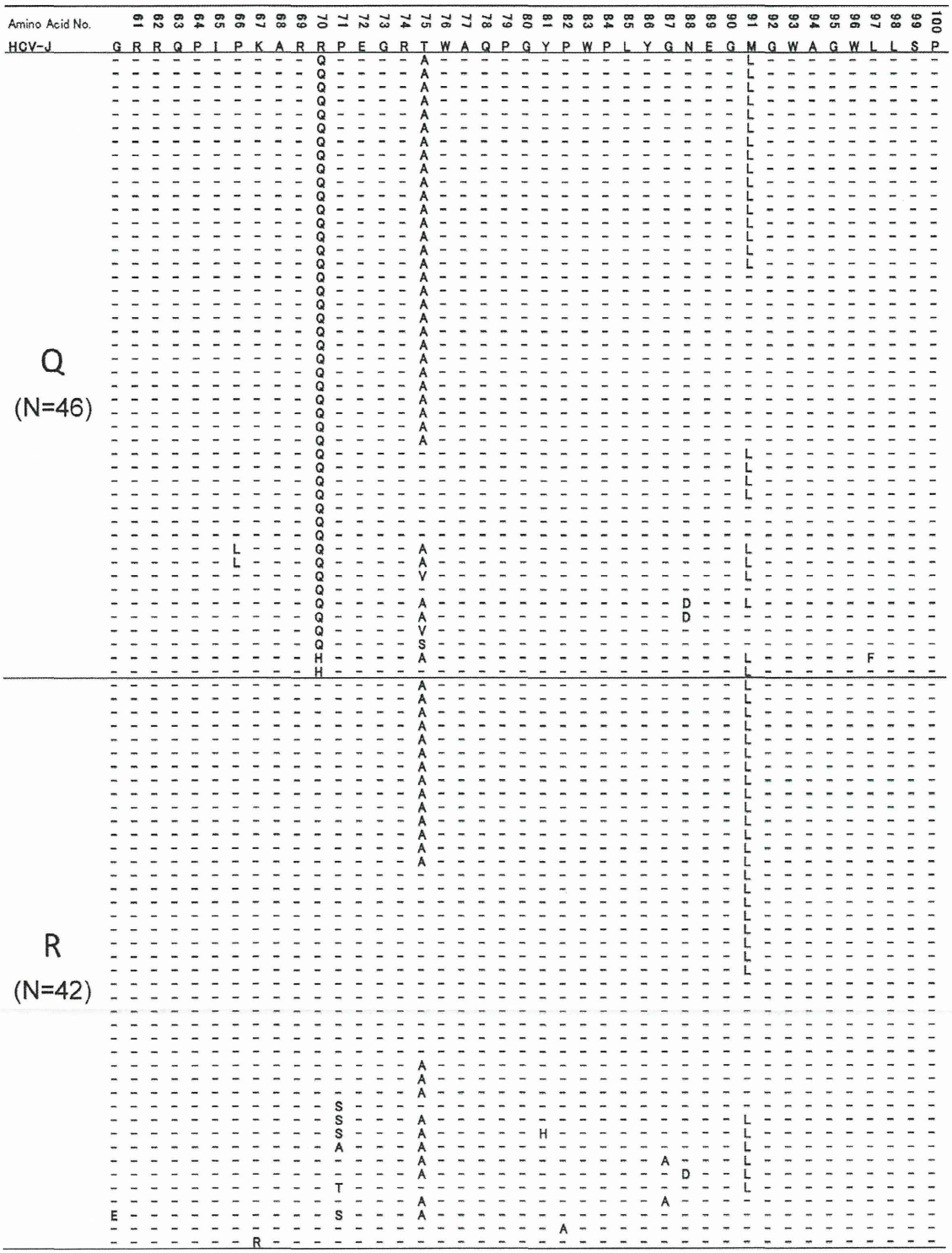

FIG 4 Dominant core amino acid haplotypic sequences dependent on the core aa 70 residues are given for all 79 patients. Two dominant sequences (a dominant core sequence in isolates with aa 70R and a dominant core sequence in isolates with aa 70non-R) were included for each of nine patients with high mixture rates (5% or more) of R and non-R at core aa 70, while one dominant sequence each was included for other patients. Therefore, a total of 88 haplotypic sequences are shown here. Since most amino acid mutations were observed in the limited core region, only that part of the core sequence is shown. The HCV-J isolate is used as the reference sequence for the core region.

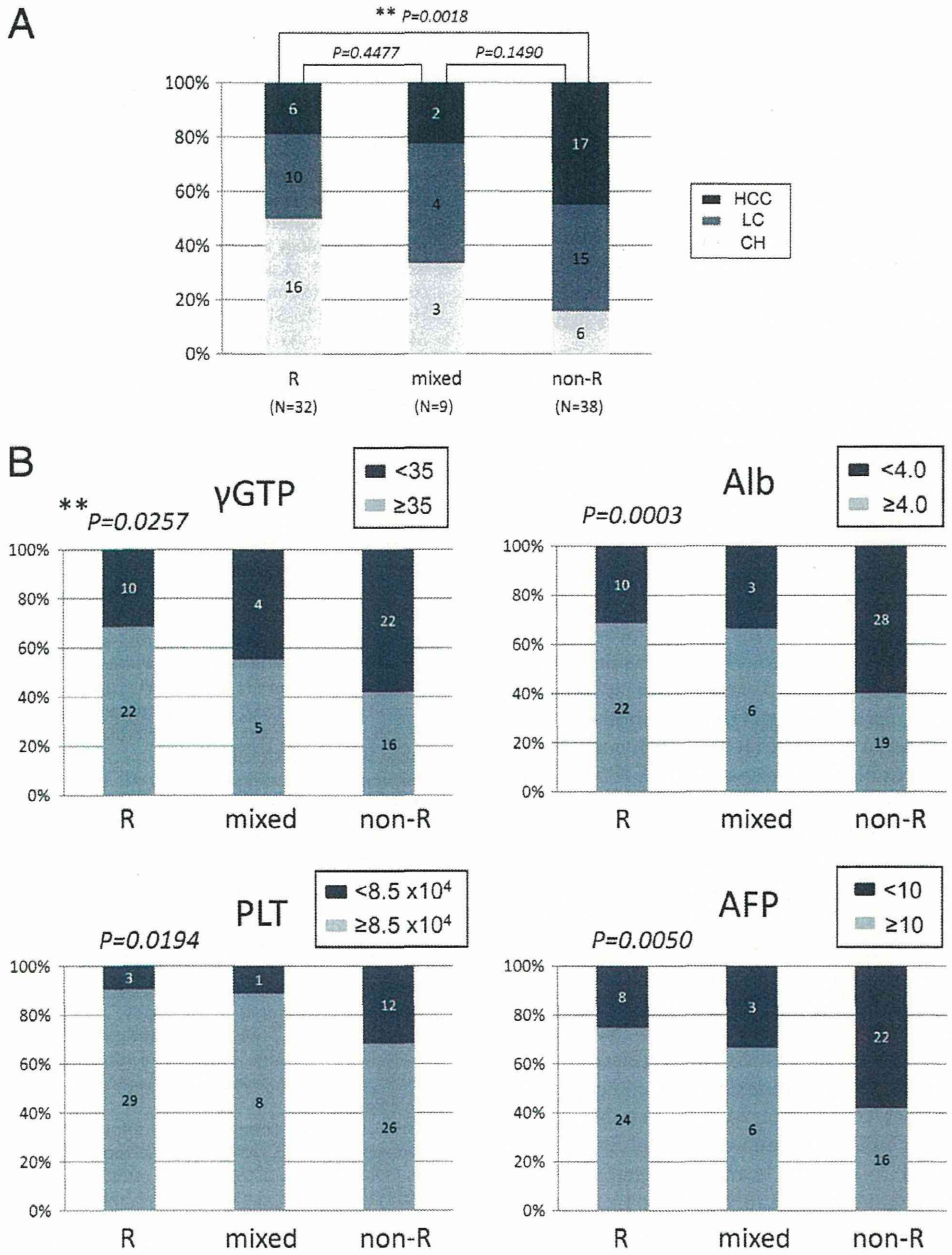

FIG 5 The advance of liver disease (A) and the levels of γ-GTP, albumin (Alb), platelets (PLT), and alpha-fetoprotein (AFP) (B) were investigated for correlation with the ratio of R to non-R at core aa 70. Results for R/R + non-R ratios of ≥95% (R), ≥5% and <95% (mixed), and <5% (non-R) are shown. **, Cochran-Armitage analysis.

because the presence of a quasispecies was expected at this position, considering reports by previous studies of its association with liver disease progression and the frequent observation of time-dependent changes (8, 9). R and non-R residues were mixed in 89.9% of the 79 patients examined in this study, indicating that the absence of a mixture was rare. Furthermore, the percentage of total isolates encoding non-R residues at this position showed a relationship with the advance of chronic liver disease, as shown in Fig. 2A and Table 3. Therefore, with regard to the relationship between the advance of liver disease and core aa 70, it may be accurate to say that a change in the ratio of amino acids at core aa 70, rather than mutation of core aa 70, was related to the advance of liver disease.

Because information for almost the entire core region was obtained from each patient, our next interest was to determine whether core aa 70 is associated with other viral regions. In other words, we sought to determine whether HCVs with core aa 70R and HCVs with core aa 70non-R are phylogenetically distinct variants. To clarify the issue, phylogenetic tree analysis using dominant sequences for the (almost-entire) core regions from all 79 patients was performed at first. This analysis disclosed, after the calculation of genetic distances, that core sequences with aa

70non-R were significantly more homogeneous than those with aa 70R, demonstrating that the hot spot core aa 70 residue is significantly associated with the remainder of the core sequence. Although the underlying mechanism is unclear, we speculated that the close correlation between core aa 70 residues and IL28B SNPs might have contributed to the result. That is, since endogenous IFN levels are known to be upregulated in patients with IL28B minor types (TG/GG) relative to those in patients with the IL28B major type (TT) in its natural state (28), it is possible that HCVs with core aa 70non-R, which are closely linked to IL28B TG/GG, are under strong antiviral pressure induced by IFN, resulting in the selection of more-homogeneous HCVs, which can survive in such an environment.

Considering this possibility, we proceeded to perform phylogenetic analyses of core sequences in single patients with high-percentage mixtures (5% or more) of R and non-R residues at core aa 70 by using deep-sequencing data, since the influence of endogenous IFNs was considered equal for all HCV isolates in a single patient. The deep-sequencing data showed that the genetic heterogeneity of core sequences in a single patient did not differ according to the core aa 70 residue but that core sequences formed distinct subgroups on the phylogenetic tree according to the core aa 70 residue (Fig. 3B), and this result was also proved by the calculation of genetic distances (Table 5). However, since no common haplotypic sequences specific to each residue at core aa 70 were found across the patients (Fig. 4), we cannot determine whether core aa 70R and aa 70non-R HCVs are phylogenetically distinct variants. It is possible that the result simply reflects a major evolutional event of core aa 70 mutations followed by derivative variants; however, extension of the investigation and analysis to viral regions beyond the core region might reveal such associations. However, due to the technical limitations of second-generation sequencers, deep-sequencing analysis of the long amplicon is difficult, and new technology is needed.

With regard to the mechanism underlying the relationship between the core protein and disease progression and hepatocarcinogenesis, a study using transgenic mice showed that the core protein induces HCC (29). Fat metabolism was accelerated in the liver, leading to inflammation, iron metabolism, oxidative stress, and insulin resistance, which were considered to be the carcinogenic factors (30–32). Clinically, mutation of the core and the concentration of γ-GTP in serum, a marker of steatosis, are related, and the relationship between IL28B SNP and liver steatosis or γ-GTP has been elucidated (33). In this study, moreover, we have confirmed the correlation between the core aa 70 mixture ratio, determined by deep-sequencing analysis, and clinical parameters reflecting disease progression, illustrating the significant association of core aa 70 with disease progression (Fig. 5A and B).

In conclusion, the quasispecies state of the core region was analyzed by deep sequencing. It was found that the status of the quasispecies was closely related to the advance of HCV-associated liver disease. In order to understand the mechanism of hepatocarcinogenesis, it is desirable to elucidate pathogenesis further by detailed examination of the quasispecies of the HCV core gene.

ACKNOWLEDGMENTS

Nobuyuki Enomoto received research funding from MSD (Tokyo, Japan) and Roche (Tokyo, Japan).

This study was supported in part by grants-in-aid from the Ministry of Education, Science, Sports and Culture of Japan (grants 23390195, 23791404, 24590964, and 24590965) and in part by grants-in-aid from the Ministry of Health, Labour, and Welfare of Japan (H23-kanen-001, H23-kanen-004, H23-kanen-006, H24-kanen-002, H24-kanen-004, and H25-kanen-006).

REFERENCES

1. Niederau C, Lange S, Heintges T, Erhardt A, Buschkamp M, Hurter D, Nawrocki M, Kruska L, Hensel F, Petry W, Haussinger D. 1998. Prognosis of chronic hepatitis C: results of a large, prospective cohort study. Hepatology 28:1687–1695.
2. Koike K. 2005. Molecular basis of hepatitis C virus-associated hepatocarcinogenesis: lessons from animal model studies. Clin. Gastroenterol. Hepatol. 3:S132–S135.
3. Akuta N, Suzuki F, Sezaki H, Suzuki Y, Hosaka T, Someya T, Kobayashi M, Saitoh S, Watahiki S, Sato J, Matsuda M, Arase Y, Ikeda K, Kumada H. 2005. Association of amino acid substitution pattern in core protein of hepatitis C virus genotype 1b high viral load and non-virological response to interferon-ribavirin combination therapy. Intervirology 48:372–380.
4. Akuta N, Suzuki F, Hirakawa M, Kawamura Y, Sezaki H, Suzuki Y, Hosaka T, Kobayashi M, Saitoh S, Arase Y, Ikeda K, Kumada H. 2011. Amino acid substitutions in hepatitis C virus core region predict hepatocarcinogenesis following eradication of HCV RNA by antiviral therapy. J. Med. Virol. 83:1016–1022.
5. Akuta N, Suzuki F, Kawamura Y, Yatsuji H, Sezaki H, Suzuki Y, Hosaka T, Kobayashi M, Arase Y, Ikeda K, Kumada H. 2007. Amino acid substitutions in the hepatitis C virus core region are the important predictor of hepatocarcinogenesis. Hepatology 46:1357–1364.
6. Fishman SL, Factor SH, Balestrieri C, Fan X, Dibisceglie AM, Desai SM, Benson G, Branch AD. 2009. Mutations in the hepatitis C virus core gene are associated with advanced liver disease and hepatocellular carcinoma. Clin. Cancer Res. 15:3205–3213.
7. Nakamoto S, Imazeki F, Fukai K, Fujiwara K, Arai M, Kanda T, Yonemitsu Y, Yokosuka O. 2010. Association between mutations in the core region of hepatitis C virus genotype 1 and hepatocellular carcinoma development. J. Hepatol. 52:72–78.
8. Akuta N, Suzuki F, Seko Y, Kawamura Y, Sezaki H, Suzuki Y, Hosaka T, Kobayashi M, Hara T, Saitoh S, Arase Y, Ikeda K, Kumada H. 2012. Complicated relationships of amino acid substitution in hepatitis C virus core region and IL28B genotype influencing hepatocarcinogenesis. Hepatology 56:2134–2141.
9. Miura M, Maekawa S, Kadokura M, Sueki R, Komase K, Shindo H, Ohmori T, Kanayama A, Shindo K, Amemiya F, Nakayama Y, Kitamura T, Uetake T, Inoue T, Sakamoto M, Okada S, Enomoto N. 2012. Analysis of viral amino acids sequences and the IL28B SNP influencing the development of hepatocellular carcinoma in chronic hepatitis C. Hepatol. Int. 6:386–396.
10. Ge D, Fellay J, Thompson AJ, Simon JS, Shianna KV, Urban TJ, Heinzen EL, Qiu P, Bertelsen AH, Muir AJ, Sulkowski M, McHutchison JG, Goldstein DB. 2009. Genetic variation in IL28B predicts hepatitis C treatment-induced viral clearance. Nature 461:399–401.
11. Rauch A, Kutalik Z, Descombes P, Cai T, Di Iulio J, Mueller T, Bochud M, Battegay M, Bernasconi E, Borovicka J, Colombo S, Cerny A, Dufour JF, Furrer H, Gunthard HF, Heim M, Hirschel B, Malinverni R, Moradpour D, Mullhaupt B, Witteck A, Beckmann JS, Berg T, Bergmann S, Negro F, Telenti A, Bochud PY. 2010. Genetic variation in *IL28B* is associated with chronic hepatitis C and treatment failure: a genome-wide association study. Gastroenterology 138:1338–1345.e7.
12. Suppiah V, Moldovan M, Ahlenstiel G, Berg T, Weltman M, Abate ML, Bassendine M, Spengler U, Dore GJ, Powell E, Riordan S, Sheridan D, Smedile A, Fragomeli V, Muller T, Bahlo M, Stewart GJ, Booth DR, George J. 2009. IL28B is associated with response to chronic hepatitis C interferon-alpha and ribavirin therapy. Nat. Genet. 41:1100–1104.
13. Tanaka Y, Nishida N, Sugiyama M, Kurosaki M, Matsuura K, Sakamoto N, Nakagawa M, Korenaga M, Hino K, Hige S, Ito Y, Mita E, Tanaka E, Mochida S, Murawaki Y, Honda M, Sakai A, Hiasa Y, Nishiguchi S, Koike A, Sakaida I, Imamura M, Ito K, Yano K, Masaki N, Sugauchi F, Izumi N, Tokunaga K, Mizokami M. 2009. Genome-wide association of IL28B with response to pegylated interferon-alpha and ribavirin therapy for chronic hepatitis C. Nat. Genet. 41:1105–1109.
14. Bochud PY, Bibert S, Kutalik Z, Patin E, Guergnon J, Nalpas B, Goossens N, Kuske L, Mullhaupt B, Gerlach T, Heim MH, Moradpour

D, Cerny A, Malinverni R, Regenass S, Dollenmaier G, Hirsch H, Martinetti G, Gorgiewski M, Bourliere M, Poynard T, Theodorou I, Abel L, Pol S, Dufour JF, Negro F. 2012. IL28B alleles associated with poor hepatitis C virus (HCV) clearance protect against inflammation and fibrosis in patients infected with non-1 HCV genotypes. Hepatology 55:384–394.

15. Fabris C, Falleti E, Cussigh A, Bitetto D, Fontanini E, Bignulin S, Cmet S, Fornasiere E, Fumolo E, Fangazio S, Cerutti A, Minisini R, Pirisi M, Toniutto P. 2011. IL-28B rs12979860 C/T allele distribution in patients with liver cirrhosis: role in the course of chronic viral hepatitis and the development of HCC. J. Hepatol. 54:716–722.
16. Joshita S, Umemura T, Katsuyama Y, Ichikawa Y, Kimura T, Morita S, Kamijo A, Komatsu M, Ichijo T, Matsumoto A, Yoshizawa K, Kamijo N, Ota M, Tanaka E. 2012. Association of IL28B gene polymorphism with development of hepatocellular carcinoma in Japanese patients with chronic hepatitis C virus infection. Hum. Immunol. 73:298–300.
17. Marabita F, Aghemo A, De Nicola S, Rumi MG, Cheroni C, Scavelli R, Crimi M, Soffredini R, Abrignani S, De Francesco R, Colombo M. 2011. Genetic variation in the interleukin-28B gene is not associated with fibrosis progression in patients with chronic hepatitis C and known date of infection. Hepatology 54:1127–1134.
18. Pawlotsky JM. 2006. Hepatitis C virus population dynamics during infection. Curr. Top. Microbiol. Immunol. 299:261–284.
19. Hiraga N, Imamura M, Abe H, Hayes CN, Kono T, Onishi M, Tsuge M, Takahashi S, Ochi H, Iwao E, Kamiya N, Yamada I, Tateno C, Yoshizato K, Matsui H, Kanai A, Inaba T, Tanaka S, Chayama K. 2011. Rapid emergence of telaprevir resistant hepatitis C virus strain from wild-type clone in vivo. Hepatology 54:781–788.
20. Nasu A, Marusawa H, Ueda Y, Nishijima N, Takahashi K, Osaki Y, Yamashita Y, Inokuma T, Tamada T, Fujiwara T, Sato F, Shimizu K, Chiba T. 2011. Genetic heterogeneity of hepatitis C virus in association with antiviral therapy determined by ultra-deep sequencing. PLoS One 6:e24907. doi:10.1371/journal.pone.0024907.
21. Verbinnen T, Van Marck H, Vandenbroucke I, Vijgen L, Claes M, Lin TI, Simmen K, Neyts J, Fanning G, Lenz O. 2010. Tracking the evolution of multiple *in vitro* hepatitis C virus replicon variants under protease inhibitor selection pressure by 454 deep sequencing. J. Virol. 84:11124–11133.
22. Wang GP, Sherrill-Mix SA, Chang KM, Quince C, Bushman FD. 2010. Hepatitis C virus transmission bottlenecks analyzed by deep sequencing. J. Virol. 84:6218–6228.
23. Nagayama K, Kurosaki M, Enomoto N, Maekawa SY, Miyasaka Y, Tazawa J, Izumi N, Marumo F, Sato C. 1999. Time-related changes in full-length hepatitis C virus sequences and hepatitis activity. Virology 263:244–253.
24. Gates AT, Sarisky RT, Gu B. 2004. Sequence requirements for the development of a chimeric HCV replicon system. Virus Res. 100:213–222.
25. Tamura K, Peterson D, Peterson N, Stecher G, Nei M, Kumar S. 2011. MEGA5: molecular evolutionary genetics analysis using maximum likelihood, evolutionary distance, and maximum parsimony methods. Mol. Biol. Evol. 28:2731–2739.
26. Becker EA, Burns CM, Leon EJ, Rajabojan S, Friedman R, Friedrich TC, O'Connor SL, Hughes AL. 2012. Experimental analysis of sources of error in evolutionary studies based on Roche/454 pyrosequencing of viral genomes. Genome Biol. Evol. 4:457–465.
27. Quince C, Lanzen A, Curtis TP, Davenport RJ, Hall N, Head IM, Read LF, Sloan WT. 2009. Accurate determination of microbial diversity from 454 pyrosequencing data. Nat. Methods 6:639–641.
28. Honda M, Sakai A, Yamashita T, Nakamoto Y, Mizukoshi E, Sakai Y, Nakamura M, Shirasaki T, Horimoto K, Tanaka Y, Tokunaga K, Mizokami M, Kaneko S. 2010. Hepatic ISG expression is associated with genetic variation in interleukin 28B and the outcome of IFN therapy for chronic hepatitis C. Gastroenterology 139:499–509.
29. Moriya K, Fujie H, Shintani Y, Yotsuyanagi H, Tsutsumi T, Ishibashi K, Matsuura Y, Kimura S, Miyamura T, Koike K. 1998. The core protein of hepatitis C virus induces hepatocellular carcinoma in transgenic mice. Nat. Med. 4:1065–1067.
30. Leandro G, Mangia A, Hui J, Fabris P, Rubbia-Brandt L, Colloredo G, Adinolfi LE, Asselah T, Jonsson JR, Smedile A, Terrault N, Pazienza V, Giordani MT, Giostra E, Sonzogni A, Ruggiero G, Marcellin P, Powell EE, George J, Negro F. 2006. Relationship between steatosis, inflammation, and fibrosis in chronic hepatitis C: a meta-analysis of individual patient data. Gastroenterology 130:1636–1642.
31. Nishina S, Hino K, Korenaga M, Vecchi C, Pietrangelo A, Mizukami Y, Furutani T, Sakai A, Okuda M, Hidaka I, Okita K, Sakaida I. 2008. Hepatitis C virus-induced reactive oxygen species raise hepatic iron level in mice by reducing hepcidin transcription. Gastroenterology 134:226–238.
32. Okuda M, Li K, Beard MR, Showalter LA, Scholle F, Lemon SM, Weinman SA. 2002. Mitochondrial injury, oxidative stress, and antioxidant gene expression are induced by hepatitis C virus core protein. Gastroenterology 122:366–375.
33. Abe H, Ochi H, Maekawa T, Hayes CN, Tsuge M, Miki D, Mitsui F, Hiraga N, Imamura M, Takahashi S, Ohishi W, Arihiro K, Kubo M, Nakamura Y, Chayama K. 2010. Common variation of IL28 affects γ-GTP levels and inflammation of the liver in chronically infected hepatitis C virus patients. J. Hepatol. 53:439–443.

JOURNAL OF VIRAL HEPATITIS
JVH

Journal of Viral Hepatitis, 2012 doi:10.1111/j.1365-2893.2012.01649.x

IL-28B (IFN-λ3) and IFN-α synergistically inhibit HCV replication

H. Shindo,[1] S. Maekawa,[1] K. Komase,[1] M. Miura,[1] M. Kadokura,[1] R. Sueki,[1] N. Komatsu,[1] K. Shindo,[1] F. Amemiya,[1] Y. Nakayama,[1] T. Inoue,[1] M. Sakamoto,[1] A. Yamashita,[2] K. Moriishi[2] and N. Enomoto[1] [1]*First Department of Internal Medicine, University of Yamanashi, Yamanashi, Japan; and* [2]*Department of Microbiology, University of Yamanashi, Yamanashi, Japan*

Received March 2012; accepted for publication June 2012

SUMMARY. Genetic variation in the IL-28B (interleukin-28B: interferon lambda 3) region has been associated with sustained virological response (SVR) rates in patients with chronic hepatitis C treated with peginterferon-α and ribavirin. However, the mechanisms by which polymorphisms in the IL-28B gene region affect host antiviral responses are not well understood. Using the HCV 1b and 2a replicon system, we compared the effects of IFN-λs and IFN-α on HCV RNA replication. The anti-HCV effect of IFN-λ3 and IFN-α in combination was also assessed. Changes in gene expression induced by IFN-λ3 and IFN-α were compared using cDNA microarray analysis. IFN-λs at concentrations of 1 ng/mL or more exhibited concentration- and time-dependent HCV inhibition. In combination, IFN-λ3 and IFN-α had a synergistic anti-HCV effect; however, no synergistic enhancement was observed for interferon-stimulated response element (ISRE) activity or upregulation of interferon-stimulated genes (ISGs). With respect to the time course of ISG upregulation, the peak of IFN-λ3-induced gene expression occurred later and lasted longer than that induced by IFN-α. In addition, although the genes upregulated by IFN-α and IFN-λ3 were similar to microarray analysis, interferon-stimulated gene expression appeared early and was prolonged by combined administration of these two IFNs. In conclusion, IFN-α and IFN-λ3 in combination showed synergistic anti-HCV activity *in vitro*. Differences in time-dependent upregulation of these genes might contribute to the synergistic antiviral activity.

Keywords: HCV, IFN-λ, IL-28B, ISG, synergistic inhibition, microarray.

INTRODUCTION

In 2009, reports from three genome-wide association studies revealed that several single-nucleotide polymorphisms (SNPs) (rs12979860, rs12980275 and rs8099917) around the IL-28B (interleukin-28B: interferon lambda 3) gene are strongly associated with sustained viral response (SVR) to PEG-IFN and RBV treatment for chronic hepatitis C [1–3]. Specifically, patients with the TG or GG genotype at rs8099917 infected with genotype 1b are more resistant to PEG-IFN and RBV treatment than patients with the TT genotype. IL-28B haplotypes were also reported to be strongly associated with spontaneous HCV clearance [1, 4, 5].

IL-28B is a member of the type III IFN family [6], consisting of IFN-λ1 (IL-29), IFN-λ2 (IL-28A) and IFN-λ3 (IL-28B). IFN-λs bind to their cognate receptor, composed of IL28R1 and IL10R2, and then activate the receptor-associated Janus-activated kinases (Jak) 1 and tyrosine kinase (Tyk) 2, leading to the activation of downstream signal transducer and activator of transcription (STAT) proteins, STAT1 and STAT2. Similar to type I IFN signalling, the Jak-STAT signalling pathway activates the IFN-stimulated response element (ISRE) within the promoter region of interferon-stimulated genes (ISGs) [7].

Concerning the functional role of IL-28B in HCV infection, two of *in vivo* studies assessed the correlation of IL-28A/B mRNA levels in whole blood and peripheral blood mononuclear cells (PBMC) with IL-28B haplotypes at position rs8099917. IL-28A mRNA and IL-28B mRNA levels in subjects with the TT genotype were higher than in subjects with other genotypes (TG or GG), suggesting an association between higher amounts of endogenous IFN-λs and HCV clearance [2, 3]. On the other hand, subjects

Abbreviations: DMEM, Dulbecco's modified Eagle's medium; FBS, foetal bovine serum; ISG, interferon-stimulated genes; MTS, dimethylthiazol carboxymethoxyphenyl sulphophenyl tetrazolium; PBMC, peripheral blood mononuclear cells; SNP, single-nucleotide polymorphisms; STAT, signal transducer and activator of transcription; SVR, sustained viral response.

Correspondence: Shinya Maekawa, M.D., Ph.D., First Department of Internal Medicine, University of Yamanashi, 1110, Shimokato, Chuo, Yamanashi 409-3898, Japan. E-mail: maekawa@yamanashi.ac.jp

with the TT genotype at SNP rs8099917 were reported to have lower expression levels of ISGs in the liver during the pretreatment period as compared with subjects with the TG or GG genotypes [8]. Several *in vitro* studies support a direct role of IFN-λs in the control of HCV replication through the innate immune pathway. In a cell culture system, Marcello *et al.* [9] showed that IFN-λ1 inhibited HCV replication with similar kinetics to that of IFN-α, although IFN-λ1 induced stronger upregulation of ISGs and this effect lasted longer. Moreover, combinations of IFN-λ1 and IFN-α had a greater inhibitory effect on HCV replication compared with the individual agents [10].

As suggested by the studies performed to date, a change in IFN-λ3 expression might be a key mechanism by which IL-28B SNPs determine the response to PEG-IFN and RBV. Considering that IFN-λ1 plays a direct role in the control of HCV replication and that IFN-λ1 enhances the antiviral activity of IFN-α, it seems reasonable to speculate that IFN-λ3 plays a similar antiviral role. Therefore, in this study, we investigated the direct antiviral role of IFN-λ3 alone and in combination with IFN-α using an HCV replicon system. In addition, we used microarray analysis to investigate the influence of IFN-λ3, alone or in combination with IFN-α, on the regulation of ISG-mediated antiviral pathways.

MATERIALS AND METHODS

Cell culture and HCV replicon

The human hepatoma cell lines OR6 and Huh7.5.1 were maintained in Dulbecco's modified Eagle's medium (DMEM: Sigma, St. Louis, MO, USA) supplemented with 10% foetal bovine serum (FBS) at 37°C in 5% CO_2. JFH-1-infected Huh7.5.1 cells were grown in DMEM supplemented with 10% FBS. The OR6 cell line, harbouring full-length genotype 1b HCV RNA and co-expressing *Renilla* luciferase (ORN/C-5B/KE) [11], was established in the presence of 500 μg/mL G418 (Promega, Madison, WI, USA).

Reagents

IL-28A (IFN-λ2), IL-28B (IFN-λ3) and IL-29 (IFN-λ1) were obtained from R&D Systems (Minneapolis, MN, USA). IL-28A and IL-29 are recombinant proteins generated from an NSO-derived murine myeloma cell line, and IL-28B is a recombinant protein generated from the CHO cell line. Interferon alpha-2b (INTRON®A 300 IU) was obtained from Schering-Plough Corporation (Kenilworth, NJ, USA).

Reporter plasmids and luciferase assay

HCV replication in OR6 replicon cells was determined by monitoring *Renilla* luciferase activity (Promega). To monitor IFN signalling directed by the interferon-stimulated response element (ISRE), the plasmids pISRE-luc expressing firefly luciferase were cotransfected using FuGENE®6 Transfection Reagent (Roche, Indianapolis, IN, USA) following the manufacturer's protocol. Luciferase activity was quantified using the dual-luciferase assay system (Promega) and a GloMax 96 Microplate Luminometer (Promega). Assays were performed in triplicate, and the results were expressed as mean ± SD percentage of the control values.

Quantification of HCV core protein and RNA

We quantified HCV core protein in culture supernatant using Lumipulse Ortho HCV Ag (Ortho Clinical Diagnostics, Tokyo, Japan) as specified by the manufacturer. The principle of the measurement method is based on the chemiluminescent enzyme immunoassay (CLEIA) [12].

Real-time reverse transcription polymerase chain reaction (RT-PCR)

Intracellular genomic JFH-1 HCV RNA as well as cellular mRNA of IFI-6, IFIT1 (ISG56), DDX60, OAS2, Mx1 and USP18 was quantified by TaqMan RT-PCR. The cells were lysed and subjected to reverse transcription without purification of RNA using a Cells-to-Ct kit (Applied Biosystems, Foster City, CA, USA) according to the manufacturer's protocol. Quantitative PCR was performed in triplicate using a 7500 Real-Time PCR System (Applied Biosystems) and TaqMan Gene Expression Assays (Applied Biosystems) according to the manufacturer's instructions. The sequences of the sense and antisense primers and the TaqMan probe for 5'UTR region of HCV were 5'-TGCGG AACCGGTGAGTACA-3', 5'-CTTAAGGTTTAGGATTCGTGCT CAT-3' and 5'-(FAM)CACCCTATCAGGCAGTACCACAAGG CC(TAMRA)-3', respectively. TaqMan probes for IFI-6, IFIT1 (ISG56), DDX60, OAS2, Mx1 and USP18 were purchased from Applied Biosystems. Primers for 18s rRNA (Applied Biosystems) were used as internal control.

Microarray analysis

OR6 replicon cells were harvested by centrifugation after exposure to 0.01 ng/mL IFN-α, 10 ng/mL IFN-λ3 or a combination of both for 6, 12, 24 and 48 h. Total RNA was isolated from cells using the RNeasy Mini Kit (Qiagen, Valencia, CA, USA). On-column DNase digestion was performed using the RNase-Free DNase Set (Qiagen). Quality control of extracted RNA was performed with the 2100 Bioanalyzer (Agilent Technologies, Palo Alto, CA, USA).

The RNA was then amplified and labelled using the Ambion® WT Expression Kit and GeneChip® WT Terminal Labelling and Control Kit (Affymetrix, Santa Clara, CA, USA). cDNA was synthesized, labelled and hybridized to the GeneChip® array according to the manufacturer's protocol, starting with 200-ng total RNA. The GeneChips were finally washed

and stained using the GeneChip® Fluidics Station 450 (Affymetrix) and then scanned with the GeneChip® Scanner 3000 7G (Affymetrix).

Affymetrix CEL files were imported into GeneSpring GX v.11.5 (Agilent Technologies, Santa Clara, CA, USA) analysis software. Data were normalized using robust multichip average analysis (RMA).

Dimethylthiazol carboxymethoxyphenyl sulphophenyl tetrazolium (MTS) assays

To evaluate the cell viability, dimethylthiazol carboxymethoxyphenyl sulphophenyl tetrazolium (MTS) assays were performed using a CellTiter 96 AQueous One Solution Cell Proliferation Assay kit (Promega) according to the manufacturer's instructions.

Statistical analyses

Statistical analyses were performed using an unpaired, two-tailed Student's *t*-test. *P* values of < 0.05 were considered to be statistically significant.

RESULTS

IFN-λ1, IFN-λ2 and IFN-λ3 demonstrate antiviral activity against HCV

To determine the antiviral effect of IL-29 (IFN-λ1), IL-28A (IFN-λ2) and IL-28B (IFN-λ3) against HCV, OR6/ORN/C-5B/KE cells were seeded in 96-well plates for 24 h and then treated with IFN-λ1, IFN-λ2, IFN-λ3 or IFN-α at various concentrations for another 24, 48 and 72 h. In this system, the *Renilla* luciferase activity reflects the amount of HCV RNA synthesized. As shown in Fig. 1, at concentrations of 1 ng/mL or more, all IFN-λs led to a concentration- and time-dependent decrease in luciferase activity of the OR6/C-5B replicon. IFN-λ3 at 10 ng/mL inhibited HCV replication (32% reduction, $P < 0.05$) to a similar extent as 0.01 ng/mL IFN-α (49% reduction, $P < 0.05$) by 48 h.

We also assessed the effects of IFN-λ1, IFN-λ2 and IFN-λ3 on Huh7.5.1/JFH-1 cells. JFH-1 cells were seeded in 96-well plates for 24 h and then treated with IFN-λ1, IFN-λ2, IFN-λ3 or IFN-α at various doses for another 48 h. To determine their antiviral effect, HCV core protein in the medium and intracellular HCV RNA were measured by CLEIA and quantitative real-time RT-PCR, respectively. HCV RNA quantitative PCR assays were multiplexed for 18s ribosomal RNA to control for the amount of input RNA. As shown in Fig. 2, all IFN-λs inhibited HCV replication in JFH-1 cells in a concentration-dependent manner. Similarly, all of the IFN-λs caused suppression of HCV core protein secretion into the cell culture medium (Figure S1).

In C-5B system, there was no evident cytotoxicity below 100 ng/mL in any interferons except for IFN-λ1 (Figure S2). On the other hand, cytotoxicity was observed in lesser concentrations by those IFNs in JFH-1 system. However, as demonstrated in Fig. 2 and Figure S3, antiviral effect exceeded the cytotoxicity in the JFH-1 system.

Synergistic inhibition of HCV replication by IFN-λ3 and IFN-α in combination

We examined whether the combination of IFN-λ3 and IFN-α induces greater antiviral activity as compared with the individual cytokines alone. OR6/ORN/C-5B/KE cells were treated with the combinations of IFN-λ3 and IFN-α at various concentrations for 48 h. As shown in Fig. 3a, the relative concentration–inhibition curves of IFN-α were plotted for each fixed concentration of IFN-λ3, and the curves shifted to the left with increasing concentrations of IFN-λ3. The results indicate a synergistic effect of IFN-λ3 and IFN-α against HCV replication. We confirmed the synergistic effect of IFN-λ3 and IFN-α by isobologram (Fig. 3b). The inhibitory effects of the combination were quantified according to the method of Chou *et al.* using the CalcuSyn software program (Biosoft, Cambridge, UK). At the ED_{50} of each drug, the combination index was 0.40-0.61, indicating significant synergism. We also assessed the effect of the combination on Huh7.5/JFH-1 cells by HCV RNA quantitative PCR assays and HCV core protein secretion. At the ED_{50} of each drug, the combination index was 0.55 and 0.48, respectively (Table S1). The cytotoxicity was not observed at the range of concentration tested (Fig. S2E, S3E).

IFN-λ3 induces ISRE promoter activity

We used the ISRE luciferase reporter assay to assess activity downstream of the JAK-STAT signalling pathway. The ISRE-firefly luciferase plasmid was transfected into OR6/ORN/C-5B/KE cells for 24 h, and these cells were cultured with various concentrations of IFN-λ3 and IFN-α for another 12, 24 or 48 h. Firefly and *Renilla* luciferase activity was then measured.

IFN-λ3 induced ISRE luciferase activity in a time-dependent manner: activity was elevated threefold after treatment with 100 ng/mL IFN-λ3 for 48 h (Fig. 4). In contrast, IFN-α induced ISRE luciferase more rapidly, producing maximal activation of the response to IFN-α at 12 h. The combination of IFN-λ3 and IFN-α induced ISRE luciferase activity similarly to IFN-λ3 alone.

IFN-α and IFN-λ3 induce expression of similar genes in HCV 1b replicon cells

OR6/ORN/C-5B/KE cells were stimulated for 6, 12, 24 and 48 h with 0.01 ng/mL IFN-α, 10 ng/mL IFN-λ3 or a combination of both, while controls were left unstimulated for the same time interval. Induction of gene expression by IFNs was analysed in microarray experiments.

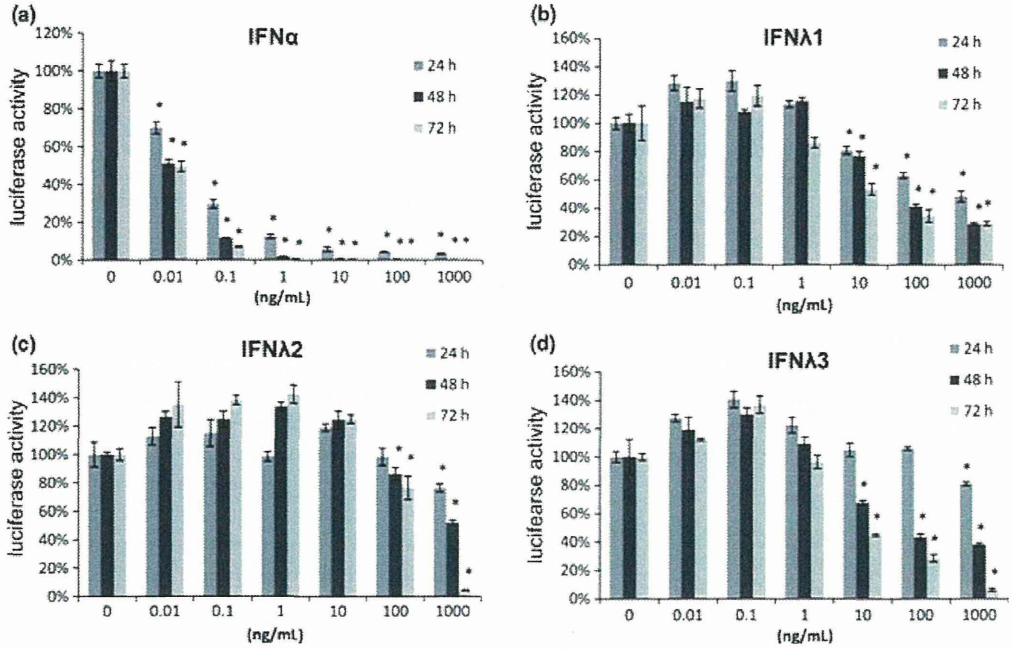

Fig. 1 IFN-α and IFN-λs inhibit HCV replicon in OR6 cells. Specific inhibition of the replication of a full-length HCV genotype 1b replicon by (a) IFN-α and (b) IFN-λ1. (c) IFN-λ2. (d) IFN-λ3 were quantified on the basis of luciferase activity. Symbols show the mean value of triplicate wells; error bars show the SD. *: $P < 0.05$ *vs* control (IFN 0 ng/mL) of each time point.

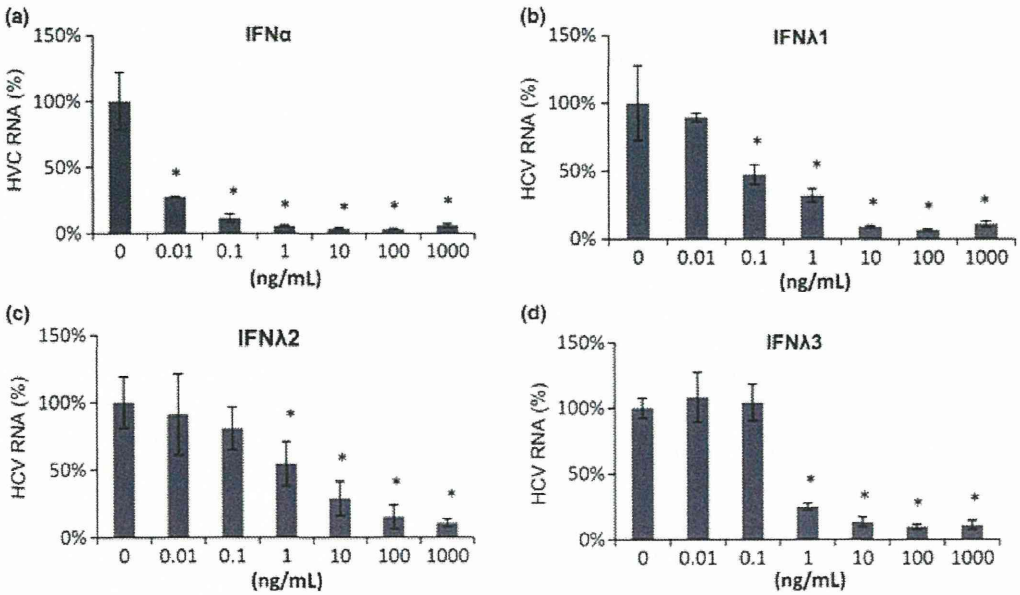

Fig. 2 IFN-α and IFN-λs inhibit HCV replicon in Huh7.5.1 cells. JFH1-infected Huh7.5.1 cells were incubated with various concentrations of (a) IFN-α and (b) IFN-λ1. (c) IFN-λ2. (d) IFN-λ3. After 48 h of treatment, total RNA was isolated and reverse transcribed, after which quantitative PCR was performed. Symbols show the mean value of triplicate wells; error bars show the SD. *: $P < 0.05$ *vs* control (IFN 0 ng/mL).

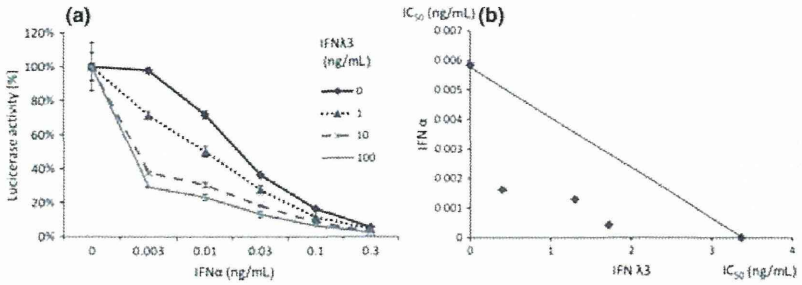

Fig. 3 Synergistic inhibitory effect of IFN-λ3 with IFN-α on hepatitis C virus replication. OR6/ORN/C-5B/KE cells were treated with combinations of IFN-λ3 with IFN-α at various concentrations. (a) The relative concentration–inhibition curves of IFN-α plotted for each fixed concentration of IFN-λ3 (0, 1, 10 and 100 ng/mL). (b) Classic isobologram for IC_{50} of IFN-λ3 with IFN-α in combination.

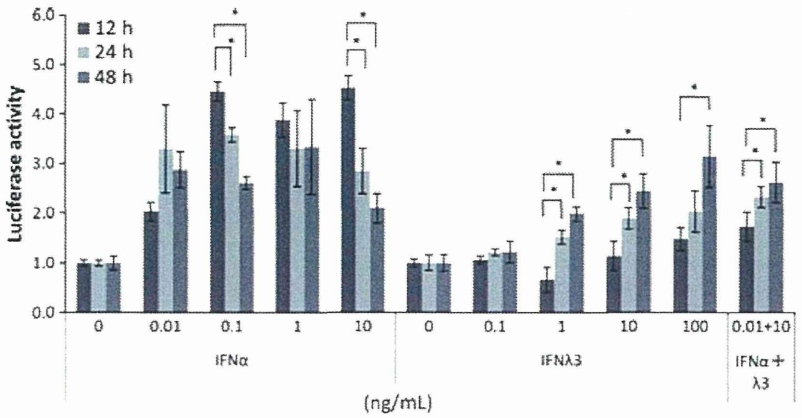

Fig. 4 IFN-stimulated response element (ISRE) promoter activity induced by IFN-α, IFN-λ3 or combination of IFN-α and IFN-λ3. OR6/ORN/C-5B/KE cells transfected with ISRE-firefly luciferase were cultured with various concentrations of IFN-α alone, IFN-λ3 alone or 0.01 ng/mL IFN-α plus 10 ng/mL IFN-λ3. ISRE-firefly luciferase activity at 24 h after transfection. Symbols show the mean value of triplicate wells; error bars show the SD. *: $P < 0.05$.

At all time points, the IFN-λ3-treated samples showed a tendency for the induction of a larger number of genes than samples treated with IFN-α. However, as shown in Table 1 listing the top 25 genes that were upregulated by both IFN-α and IFN-λ3 at 12 h, most of the upregulated genes are previously identified ISGs and the genes with high ranks were similar irrespective of the type of IFN or time point.

The time course of ISGs regulation differs between IFN-α and IFN-λ3

By microarray analysis, ISGs were more rapidly induced after the addition of IFN-α *vs* IFN-λ3 (data not shown). To confirm the rapid induction of ISGs by IFN-α, six ISGs, that is, IFI-6, IFIT1 (ISG56), DDX60, OAS2, Mx1 and USP18, were quantified for time-dependent expressional change by real-time RT-PCR. Expression of most of the genes upregulated by IFN-α peaked at 12 h and fell thereafter. In contrast, expression of IFN-λ3-induced genes peaked at 24 h and lasted up to 48 h. Combination of IFN-α and IFN-λ3 induced ISG with peak effects occurring at 12–24 h and lasting up to 48 h (Fig. 5).

DISCUSSION

In this study, we demonstrated that IFN-λ family members have distinctive time-dependent antiviral activities in an HCV replicon system and that IFN-λ3 and IFN-α have a synergistic effect in combination. Moreover, we attempted to identify the antiviral mechanism of IFN-λ3 by conducting a cDNA microarray analysis.

In previous studies, anti-HCV activity of IFN-λ1, IFN-λ2 and IFN-λ3 was reported in JFH-1 and OR6/C-5B systems [13]. Time-dependent anti-HCV activity has also been observed with IFN-λ1 [9]. In this study, we confirmed the previous results and added the further finding that time-dependent antiviral activity is not limited to IFN-λ1, but rather is common among all IFN-λs.

Table 1 Top 25 genes that were upregulated by both IFN-α and IFN-λ3 at 12 h

Gene bank ID	Gene symbol	Gene description	IFN-α 0.01 ng/mL fold increase	IFN-λ3 10 ng/mL fold increase	IFN-α+IFN-λ3 fold increase
BC007091	IFIT1	Interferon-induced protein with tetratricopeptide repeats 1	4.01	4.49	4.87
BC049215	OAS2	2′-5′-oligoadenylate synthetase 2, 69/71kDa	3.06	3.88	4.48
M33882	MX1	Myxovirus (influenza virus) resistance 1	3.24	3.29	3.69
AF095844	IFIH1	Interferon induced with helicase C domain 1	2.73	3.02	3.54
BC038115	DDX60	DEAD (Asp-Glu-Ala-Asp) box polypeptide 60	2.70	2.92	3.51
BC011601	IFI6	Interferon, alpha-inducible protein 6	3.07	3.24	3.42
BC042047	HERC6	Hect domain and RLD 6	2.56	2.75	3.34
AF442151	RSAD2	Radical S-adenosyl methionine domain containing 2	1.32	2.59	3.28
U34605	IFIT5	Interferon-induced protein with tetratricopeptide repeats 5	2.47	2.91	3.25
AY730627	OAS1	2′,5′-oligoadenylate synthetase 1, 40/46kDa	2.32	2.57	3.05
AB006746	PLSCR1	Phospholipid scramblase 1	2.37	2.51	3.03
AF307338	PARP9	Poly (ADP-ribose) polymerase family, member 9	2.39	2.46	2.94
M87503	IRF9	Interferon regulatory factor 9	2.61	2.59	2.85
AK297137	IFIT3	Interferon-induced protein with tetratricopeptide repeats 3	1.90	2.36	2.79
AK290655	EIF2AK2	Eukaryotic translation initiation factor 2-alpha kinase 2	2.47	2.45	2.77
BX648758	PARP14	Poly (ADP-ribose) polymerase family, member 14	2.07	2.25	2.66
BC132786	DDX58	DEAD (Asp-Glu-Ala-Asp) box polypeptide 58	1.83	2.17	2.59
AF445355	SAMD9	Sterile alpha motif domain containing 9	2.07	2.08	2.56
	DDX60L	DEAD (Asp-Glu-Ala-Asp) box polypeptide 60-like	1.63	1.92	2.39
BC014896	USP18| USP41	Ubiquitin-specific peptidase 18/ubiquitin-specific peptidase 41	1.52	1.78	2.11
AB044545	OAS3	2′-5′-oligoadenylate synthetase 3, 100kDa	1.44	1.57	2.10
BC010954	CXCL10	Chemokine (C-X-C motif) ligand 10	0.76	1.66	1.99
BC014896	USP18	Ubiquitin-specific peptidase 18	1.33	1.55	1.99
AL832618	IFI44L	Interferon-induced protein 44-like	0.58	1.31	1.95

We also assessed whether IFN-λ3 and IFN-α in combination could produce additive or synergistic effects on antiviral activity. In previous studies, additive antiviral activity against HCV was reported with the combination of IFN-λ1 and IFN-α [9, 10]. However, there have been no previous reports on the combined effects of IFN-λ3 and IFN-α. In this study, the focus was on IFN-λ3, because IFN-λ3 is suspected to be the key molecule, mediating the effect of SNPs in the IL-28B gene region on the anti-HCV response to IFN-α. As shown in Fig. 3 and Table S1, synergistic induction of anti-HCV activity occurred in both the OR6/C-5B and Huh7.5/JFH-1 HCV replicon systems. Synergy was demonstrated by the combination index values (Table S1).

Although it has been reported that the upregulated genes induced by IFN-λ are similar to those induced by IFN-α [9, 14–16], there have been no previous reports on

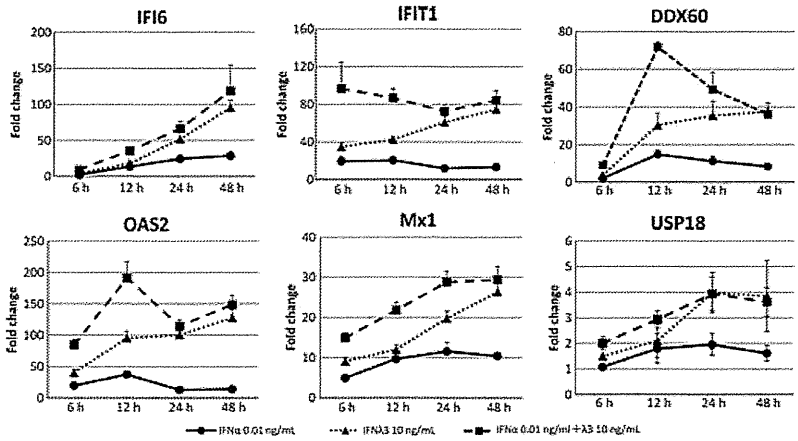

Fig. 5 Time course of ISG expression induced by 0.01 ng/mL IFN-α, 10 ng/mL IFN-λ3 or 0.01 ng/mL IFN-α plus 10 ng/mL IFN-λ3. Expression of the ISGs – IFI-6, IFIT1 (ISG56), DDX60, OAS2, Mx1 and USP18 – in OR6/ORN/C-5B/KE cells treated 6, 12, 24 and 48 h were determined by qRT-PCR. Results are presented as the relative fold induction. Symbols show the mean value of triplicate wells; error bars show the SD. *Solid lines* represent 0.01 ng/mL IFN-α alone, whereas *fine dashed lines* show 10 ng/mL IFN-λ3 alone, and *coarse dashed lines* show the combination of the 2 cytokines.

the genes induced by IFN-α and IFN-λ in combination. In cDNA microarray analysis, as demonstrated in Table 1, the most strongly upregulated genes induced by IFN-α/IFN-λ3 alone or in combination were almost identical, and most of them were ISGs. As no genes showed upregulation specific to IFN-λ3, we speculate that IFN-α and IFN-λ3 share a similar antiviral intracellular mechanism at the molecular level.

Unexpectedly in microarray analyses, synergistic upregulation of ISGs was not observed. In the same manner, TaqMan real-time RT-PCR analysis showed that the combination of IFN-α and IFN-λ3 did not upregulate ISGs synergistically (Fig. 5). In addition to cDNA microarray analysis, ISRE reporter assays were performed to determine the activation of components of the JAK-STAT pathway common to both type I and III IFNs. As shown in Fig. 4, each IFN upregulated ISRE activity, and the combination of IFN-λ3 and IFN-α did not synergistically enhance ISRE activity either.

Meanwhile, the peak time of the induction of ISG expression differs for IFN-α and IFN-λ1 [9, 17]; peak gene expression occurs earlier with IFN-α than with IFN-λ1. In our study, we confirmed that the peak induction of gene expression occurred later (24 h) and lasted longer (24–48 h) with IFN-λ3 than with IFN-α (12 h). Importantly, gene expression appeared early (12 h) and was prolonged (48 h) by the combination of both IFNs. Similarly to the peak time difference between IFN-α and IFN-λ3 seem for ISG expression, a time-dependent increase in ISRE activation was observed with the combination of both IFNs. While the precise mechanism remains to be clarified, differential regulation of the time-dependent induction of ISG gene expression could be one of the mechanisms underlying the synergistic antiviral effect. One of the molecules contributing to time-dependent ISG upregulation is the ISG known as ubiquitin-specific peptidase 18 (USP18), which has been reported to bind to IFNAR2 and inhibit the interaction of Jak1 with its receptor, thereby preventing IFN-α signalling while leaving IFN-λ signalling unaffected [18, 19]. Actually, expression of USP18 is specifically upregulated with IFN-λ3 in this study as shown in Fig. 5. If the ISGs upregulated by IFN-α are downregulated by USP18, it is plausible that the expression of genes induced by IFN-α decreases early, while expression of genes induced by IFN-λ lasts longer.

A number of clinical studies have confirmed that SNPs around the IL-28B gene are associated with the response to PEG-IFN and RBV therapy, and as previously indicated, various investigations have been performed to clarify the underlying mechanism. Specifically, increased IL-28B mRNA expression in PBMC [2, 3], high serum concentrations of IFN-λ1 (IL-29) [20], low expression of ISGs in the liver prior to IFN treatment [8, 21] and high upregulation of ISG expression by IFN treatment [8, 22] were found in subjects with IL-28B SNP genotypes associated with SVR (rs12979860 CC and rs8099917 TT). Although the functional role of IFN-λ3 still needs to be investigated more thoroughly, if IFN-λ3 expression change is the essential difference in determining the clinical treatment response to PEG-IFN and RBV therapy and if its expression is decreased in patients with the specific IL-28B genotype, which is associated with non-SVR, it is possible that exogenous administration of IFN-λ3 might improve IFN-α-induced viral clearance and that such treatment would be beneficial for patients with the IFN-resistant IL-28B genotype.

In present study, the OR6-cultured cells harboured the rs8099917 TT genotype, and recombinant IFN-λ3 (IL-

28B) protein used in the experiment was derived from cells with the rs8099917 TT genotype (data not shown). Therefore, the viral responses and/or cellular gene expression change in cells and/or proteins with different IL-28B genotypes *in vitro* should be determined in future studies.

In conclusion, we demonstrated that IFN-α and IFN-λ3 synergistically enhance anti-HCV activity *in vitro*. Although the ISGs upregulated by IFN-α and IFN-λ3 were similar, differences in time-dependent upregulation of these genes, especially prolonged ISGs expression by IFN-λ3, might contribute to their synergistic antiviral activity.

ACKNOWLEDGEMENTS

We are grateful to Ms. Sakamoto, Ms. Endo and Mr. Osada, laboratory technicians at University of Yamanashi Hospital, for quantification of HCV core protein in culture supernatant. This study was supported in part by a grant-in-aid scientific research fund of the Ministry of Education, Science, Sports and Culture number 21590836, 21590837, 23390195 and in part by a grant-in-aid from the Ministry of Health, Labour and Welfare of Japan (H22-kanen-006).

CONFLICT OF INTEREST

Shinya Mackawa and Taisuke Inoue belong to a donation-funded department that is funded by MSD co. ltd.

REFERENCES

1 Ge D, Fellay J, Thompson AJ, *et al.* Genetic variation in IL28B predicts hepatitis C treatment-induced viral clearance. *Nature* 2009; 461: 399–401.
2 Tanaka Y, Nishida N, Sugiyama M, *et al.* Genome-wide association of IL28B with response to pegylated interferon-alpha and ribavirin therapy for chronic hepatitis C. *Nat Genet* 2009; 41: 1105–1109.
3 Suppiah V, Moldovan M, Ahlenstiel G, *et al.* IL28B is associated with response to chronic hepatitis C interferon-alpha and ribavirin therapy. *Nat Genet* 2009; 41: 1100–1104.
4 Thomas DL, Thio CL, Martin MP, *et al.* Genetic variation in IL28B and spontaneous clearance of hepatitis C virus. *Nature* 2009; 461: 798–801.
5 Rauch A, Kutalik Z, Descombes P, *et al.* Genetic variation in IL28B is associated with chronic hepatitis C and treatment failure: a genome-wide association study. *Gastroenterology* 2010; 138:1338–1345, 1345 e1331-1337.
6 Dellgren C, Gad HH, Hamming OJ, Melchjorsen J, Hartmann R. Human interferon-lambda3 is a potent member of the type III interferon family. *Genes Immun* 2009; 10: 125–131.
7 Kotenko SV, Gallagher G, Baurin VV, *et al.* IFN-lambdas mediate antiviral protection through a distinct class II cytokine receptor complex. *Nat Immunol* 2003; 4: 69–77.
8 Honda M, Sakai A, Yamashita T, *et al.* Hepatic ISG expression is associated with genetic variation in interleukin 28B and the outcome of IFN therapy for chronic hepatitis C. *Gastroenterology* 2010; 139: 499–509.
9 Marcello T, Grakoui A, Barba-Spaeth G, *et al.* Interferons alpha and lambda inhibit hepatitis C virus replication with distinct signal transduction and gene regulation kinetics. *Gastroenterology* 2006; 131: 1887–1898.
10 Pagliaccetti NE, Eduardo R, Kleinstein SH, Mu XJ, Bandi P, Robek MD. Interleukin-29 functions cooperatively with interferon to induce antiviral gene expression and inhibit hepatitis C virus replication. *J Biol Chem* 2008; 283: 30079–30089.
11 Ikeda M, Abe K, Dansako H, Nakamura T, Naka K, Kato N. Efficient replication of a full-length hepatitis C virus genome, strain O, in cell culture, and development of a luciferase reporter system. *Biochem Biophys Res Commun* 2005; 329: 1350–1359.
12 Aoyagi K, Ohue C, Iida K, *et al.* Development of a simple and highly sensitive enzyme immunoassay for hepatitis C virus core antigen. *J Clin Microbiol* 1999; 37: 1802–1808.
13 Zhang L, Jilg N, Shao RX, *et al.* IL28B inhibits hepatitis C virus replication through the JAK-STAT pathway. *J Hepatol* 2011; 55: 289–298.
14 Ank N, West H, Bartholdy C, Eriksson K, Thomsen AR, Paludan SR. Lambda interferon (IFN-lambda), a type III IFN, is induced by viruses and IFNs and displays potent antiviral activity against select virus infections in vivo. *J Virol* 2006; 80: 4501–4509.
15 Zhou Z, Hamming OJ, Ank N, Paludan SR, Nielsen AL, Hartmann R. Type III interferon (IFN) induces a type I IFN-like response in a restricted subset of cells through signaling pathways involving both the Jak-STAT pathway and the mitogen-activated protein kinases. *J Virol* 2007; 81: 7749–7758.
16 Doyle SE, Schreckhise H, Khuu-Duong K, *et al.* Interleukin-29 uses a type 1 interferon-like program to promote antiviral responses in human hepatocytes. *Hepatology* 2006; 44: 896–906.
17 Maher SG, Sheikh F, Scarzello AJ, *et al.* IFNalpha and IFNlambda differ in their antiproliferative effects and duration of JAK/STAT signaling activity. *Cancer Biol Ther* 2008; 7: 1109–1115.
18 Makowska Z, Duong FH, Trincucci G, Tough DF, Heim MH. Interferon-beta and interferon-lambda signaling is not affected by interferon-induced refractoriness to interferon-alpha in vivo. *Hepatology* 2011; 53: 1154–1163.
19 Franois-Newton V, de Freitas Almeida GM, Payelle-Brogard B, *et al.*

USP18-Based Negative Feedback Control Is Induced by Type I and Type III Interferons and Specifically Inactivates Interferon α Response. *PLoS ONE* 2011; 6: e22200.
20 Langhans B, Kupfer B, Braunschweiger I, *et al.* Interferon-lambda serum levels in hepatitis C. *J Hepatol* 2011; 54: 859–865.
21 Urban TJ, Thompson AJ, Bradrick SS, *et al.* IL28B genotype is associated with differential expression of intrahepatic interferon-stimulated genes in patients with chronic hepatitis C. *Hepatology* 2010; 52: 1888–1896.
22 Abe H, Hayes CN, Ochi H, *et al.* IL28 variation affects expression of interferon stimulated genes and peg-interferon and ribavirin therapy. *J Hepatol* 2011; 54: 1094–1101.

SUPPORTING INFORMATION

Additional Supporting Information may be found in the online version of this article:

Figure S1: IFN-α and IFN-λs inhibit HCV core protein secretion. JFH1-infected Huh7.5.1 cells were incubated with various concentrations of IFN-α and IFN-λ1, -λ2, -λ3. After 48 h of treatment, HCV core protein in the medium was measured. Symbols show the mean value of triplicate wells; error bars show the SD. *: $p < 0.05$ vs. control (IFN 0ng/ml).

Figure S2: The dimethylthiazol carboxymethoxyphenyl sulfophenyl tetrazolium assay was performed after OR6/ORN/C-5B/KE cells were cultured with various concentrations of (A) IFN-α, (B) IFN-λ1, (C) IFN-λ2, (D) IFN-λ3 and (E) combination of IFN-α and IFN-λ3 for 48 h. Symbols show the mean value of triplicate wells; error bars show the SD. *: $p < 0.05$ vs. control (IFN 0ng/ml).

Figure S3: The dimethylthiazol carboxymethoxyphenyl sulfophenyl tetrazolium assay was performed after Huh7.5.1/JFH-1 cells were cultured with various concentrations of (A) IFN-α, (B) IFN-λ1, (C) IFN-λ2, (D) IFN-λ3 and (E) combination of IFN-α and IFN-λ3 for 48 h. Symbols show the mean value of triplicate wells; error bars show the SD. *: $p < 0.05$ vs. control (IFN 0ng/ml).

Table S1: Combination index after 48hr stimulation by CalucSyn.

Please note: Wiley-Blackwell are not responsible for the content or functionality of any supporting materials supplied by the authors. Any queries (other than missing material) should be directed to the corresponding author for the article.

Journal of Medical Virology 85:449–458 (2013)

Model Incorporating the *ITPA* Genotype Identifies Patients at High Risk of Anemia and Treatment Failure With Pegylated-Interferon Plus Ribavirin Therapy for Chronic Hepatitis C

Masayuki Kurosaki,[1] Yasuhito Tanaka,[2] Nao Nishida,[3] Naoya Sakamoto,[4] Nobuyuki Enomoto,[5] Kentaro Matsuura,[2] Yasuhiro Asahina,[6] Mina Nakagawa,[6] Mamoru Watanabe,[6] Minoru Sakamoto,[5] Shinya Maekawa,[5] Katsushi Tokunaga,[3] Masashi Mizokami,[7] and Namiki Izumi[1]*

[1]*Department of Gastroenterology and Hepatology, Musashino Red Cross Hospital, Tokyo, Japan*
[2]*Department of Virology, Liver Unit, Nagoya City University Graduate School of Medical Sciences, Nagoya, Japan*
[3]*Department of Human Genetics, Graduate School of Medicine, University of Tokyo, Tokyo, Japan*
[4]*Department of Gastroenterology and Hematology, Hokkaido University, Sapporo, Japan*
[5]*First Department of Internal Medicine, University of Yamanashi, Yamanashi, Japan*
[6]*Department of Gastroenterology and Hepatology, Tokyo Medical and Dental University, Tokyo, Japan*
[7]*Research Center for Hepatitis and Immunology, International Medical Center of Japan Konodai Hospital, Ichikawa, Japan*

This study aimed to develop a model for predicting anemia using the inosine triphosphatase (*ITPA*) genotype and to evaluate its relationship with treatment outcome. Patients with genotype 1b chronic hepatitis C (n = 446) treated with peg-interferon alpha and ribavirin (RBV) for 48 weeks were genotyped for the *ITPA* (rs1127354) and *IL28B* (rs8099917) genes. Data mining analysis generated a predictive model for anemia (hemoglobin (Hb) concentration <10 g/dl); the CC genotype of *ITPA*, baseline Hb <14.0 g/dl, and low creatinine clearance (CLcr) were predictors of anemia. The incidence of anemia was highest in patients with Hb <14.0 g/dl and CLcr <90 ml/min (76%), followed by Hb <14.0 g/dl and *ITPA* CC (57%). Patients with Hb ≥14.0 g/dl and *ITPA* AA/CA had the lowest incidence of anemia (17%). Patients with two predictors (high-risk) had a higher incidence of anemia than the others (64% vs. 28%, $P < 0.0001$). At baseline, the *IL28B* genotype was a predictor of a sustained virological response [adjusted odds ratio 9.88 (95% confidence interval 5.01–19.48), $P < 0.0001$]. In patients who achieved an early virological response, the *IL28B* genotype was not associated with a sustained virological response, while a high risk of anemia was a significant negative predictor of a sustained virological response [0.47 (0.24–0.91), $P = 0.026$]. For high-risk patients with an early virological response, giving >80% of the planned RBV dose increased sustained virological responses by 24%. In conclusion, a predictive model incorporating the *ITPA* genotype could identify patients with a high risk of anemia and reduced probability of sustained virological response. ***J. Med. Virol. 85:449–458, 2013.***

KEY WORDS: hemolytic anemia; ribavirin; creatinine clearance; antiviral therapy

INTRODUCTION

Hepatitis C virus (HCV) infection is a leading cause of cirrhosis and hepatocellular carcinoma worldwide [Kim, 2002]. The rate of eradication of HCV by pegylated interferon (PEG-IFN) plus ribavirin (RBV), defined as a sustained virological response, is around 50% in patients with HCV genotype 1 [Manns et al., 2001; Fried et al., 2002]. Failure of treatment is attributable to the lack of a virological response or relapse after completion of therapy. Genome-wide association studies and subsequent cohort studies

Grant sponsor: Ministry of Health, Labor and Welfare, Japan.
Conflicts of interest and financial disclosures: None reported.

*Correspondence to: Namiki Izumi, MD, PhD, Department of Gastroenterology and Hepatology, Musashino Red Cross Hospital, 1-26-1 Kyonan-cho, Musashino-shi, Tokyo 180-8610, Japan. E-mail: nizumi@musashino.jrc.or.jp

Accepted 19 November 2012
DOI 10.1002/jmv.23497
Published online 7 January 2013 in Wiley Online Library (wileyonlinelibrary.com).

have shown that single nucleotide polymorphisms (SNPs) located near the *IL28B* gene are the most important determinant of virological response to PEG-IFN/RBV therapy [Ge et al., 2009; Suppiah et al., 2009; Tanaka et al., 2009; Rauch et al., 2010]. On the other hand, among patients with a virological response, the probability of a sustained virological response decreases when the patients become intolerant to therapy because of RBV-induced hemolytic anemia and receive a reduced dose of RBV [McHutchison et al., 2002; Kurosaki et al., 2012]. Genome-wide association studies have shown that variants of the inosine triphosphatase (*ITPA*) gene protect against hemolytic anemia [Fellay et al., 2010; Tanaka et al., 2011]. These variants are associated with a reduced requirement for an anemia-related dose reduction of RBV [Sakamoto et al., 2010; Thompson et al., 2010a; Kurosaki et al., 2011d; Seto et al., 2011]. However, factors other than the *ITPA* gene also contribute to the risk of severe anemia or RBV dose reduction [Ochi et al., 2010; Kurosaki et al., 2011d] and the results of studies on the impact of the *ITPA* genotype on treatment outcome are inconsistent [Ochi et al., 2010; Sakamoto et al., 2010; Thompson et al., 2010a, 2011; Kurosaki et al., 2011d].

Data mining is a novel statistical method used to extract relevant factors from a plethora of factors and combine them to predict the incidence of the outcome of interest [Breiman et al., 1980]. Decision tree analysis, a primary component of data mining analysis, has found medical applications recently [Averbook et al., 2002; Miyaki et al., 2002; Baquerizo et al., 2003; Leiter et al., 2004; Garzotto et al., 2005; Zlobec et al., 2005; Valera et al., 2007] and has proven to be a useful tool for predicting therapeutic efficacy [Kurosaki et al., 2010, 2011a,b,c, 2012] and adverse events [Hiramatsu et al., 2011] in patients with chronic hepatitis C treated with PEG-IFN/RBV therapy. Because the results of data mining analysis are presented as a flowchart [LeBlanc and Crowley, 1995], they are easily understandable and usable by clinicians lacking a detailed knowledge of statistics.

For the general application of this genetic information in clinical practice, this study aimed to construct a predictive model of severe anemia using the *ITPA* genotype, together with other relevant factors. This study also aimed to analyze the impact of the risk of anemia on treatment outcome, after adjustment for the *IL28B* genotype. These analyses were carried out at baseline and during therapy, when the early virological response became evident.

MATERIALS AND METHODS

Patients

Data were collected from a total of 446 genotype 1b chronic hepatitis C patients who were treated with PEG-IFN alpha and RBV at five hospitals and universities throughout Japan. The inclusion criteria were: (1) infection by hepatitis C genotype 1b; (2) no co-infection with hepatitis B virus or human immunodeficiency virus; (3) no other causes of liver disease such as autoimmune hepatitis and primary biliary cirrhosis; and (4) availability of DNA for the analysis of the genetic polymorphisms of *IL28B* and *ITPA*. Patients received PEG-IFN alpha-2a (180 μg) and 2b (1.5 μg/kg) subcutaneously every week and a daily weight-adjusted dose of RBV (600 mg for patients weighing <60 kg, 800 mg for patients weighing 60–80 kg, and 1,000 mg for patients weighing >80 kg) for 48 weeks. Dose reduction or discontinuation of PEG-IFN and RBV was primarily based on the recommendations on the package inserts and the discretion of the physicians at each university and hospital. The standard duration of therapy was set at 48 weeks. No patient received erythropoietin or other growth factors for the treatment of anemia. Written informed consent was obtained from each patient, and the study protocol conformed to the ethical guidelines of the Declaration of Helsinki and was approved by the institutional ethics review committees.

Laboratory Tests

Blood samples obtained before therapy were analyzed for hematologic data, blood chemistry, and HCV RNA. Genetic polymorphisms in SNPs of the *ITPA* gene (rs1127354) and the *IL28B* gene (rs8099917) were determined using ABI TaqMan Probes (Applied Biosystems, Carlsbad, CA) and the DigiTag2 assay, respectively. Baseline creatinine clearance (CLcr) levels were calculated using the formula of Cockcroft and Gault [1976]: for males, CLcr = [(140 − age in years) × body weight in kg] ÷ (72 × serum creatinine in mg/dl) and for females, CLcr = 0.85 × [(140 − age in years) × body weight in kg] ÷ (72 × serum creatinine in mg/dl). The stage of liver fibrosis was scored according to the METAVIR scoring system: F0 (no fibrosis), F1 (mild fibrosis: portal fibrosis without septa), F2 (moderate fibrosis: few septa), F3 (severe fibrosis: numerous septa without cirrhosis), and F4 (cirrhosis). A rapid virological response was defined as undetectable HCV RNA by qualitative PCR with a lower detection limit of 50 IU/ml (Amplicor, Roche Diagnostic Systems, Pleasanton, CA) at week 4 of therapy and a complete early virological response was defined as undetectable HCV RNA at week 12. A sustained virological response was defined as undetectable HCV RNA at 24 weeks after completion of therapy. Severe anemia was defined as hemoglobin (Hb) <10 g/dl.

Statistical Analysis

Database for analysis included the following variables: age, sex, body mass index, serum aspartate aminotransferase (AST) levels, alanine aminotransferase (ALT) levels, gamma-glutamyltransferase (GGT) levels, creatinine levels, CLcr, Hb, platelet count, serum levels of HCV RNA, and the stage of liver fibrosis

TABLE I. Patients' Baseline Characteristics

Age (years)	58.6	(9.6)
Gender: male (n, %)	185	(42%)
Body mass index (kg/m^2)	23.1	(3.7)
AST (IU/L)	59.9	(53.8)
ALT (IU/L)	69.8	(53.8)
GGT (IU/L)	48.5	(41.6)
Creatinine (mg/dl)	0.7	(0.2)
Creatinine clearance (ml/min)	89.5	(23.0)
Hemoglobin (g/dl)	14	(1.4)
Platelet count (10^9/L)	154.5	(52.1)
HCV RNA > 600,000 IU/ml (n, %)	354	(79%)
Liver fibrosis: F3-4 (n, %)	108	(24%)
Initial ribavirin dose (n, %)		
600 mg/day	300	(67%)
800 mg/day	138	(31%)
1,000 mg/day	9	(2%)
Pegylated interferon (n, %)		
alpha2a 180 mcg	58	(13%)
alpha2b 1.5 mcg/kg	388	(87%)
ITPA rs1127354: CC (n, %)	317	(71%)
IL28B rs809917: TT (n, %)	311	(70%)

AST, aspartate aminotransferase; ALT, alanine aminotransferase; GGT, gamma-glutamyltransferase.
Data expressed as mean (standard deviation) unless otherwise mentioned.

(Table I). Based on these data set, a model for predicting the risk of developing severe anemia was constructed by data mining analysis using the IBM-SPSS Modeler 13 as described previously [Kurosaki et al., 2010, 2011a,b,c; Hiramatsu et al., 2011]. Briefly, the software was used to explore the database automatically to search for optimal predictors that discriminated most efficiently patients with severe anemia from those without. The software also determined the optimal cutoff values of each predictor. Patients were divided into two groups according to the predictor and each of the two groups was repeatedly divided in the same way until no significant factor remained or 20 or fewer patients were in a group.

The incidence of severe anemia, the total dose of RBV, and treatment outcome were compared between groups with high and low risks of anemia. On univariate analysis, Student's *t*-test was used for continuous variables, and Fisher's exact test was used for categorical data. Logistic regression was used for multivariate analysis. *P* values of <0.05 were considered significant. SPSS Statistics 18 was used for these analyses.

RESULTS

Predictive Model of Severe Anemia

The incidence of severe anemia in the whole cohort was 49% (Fig. 1). The best predictor of severe anemia was the baseline Hb concentration. Patients with a low baseline Hb concentration (<14 g/dl) were more likely to develop severe anemia (67%) than those with a higher Hb (>14 g/dl) (34%). The second best predictor for those patients with a baseline Hb <14.0 g/dl was CLcr. Patients with a CLcr below 90 ml/min had the highest incidence of severe anemia (76%). In those with a CLcr above >90 ml/min the incidence of severe anemia was 57% in patients with the CC allele of the *ITPA* gene while it was 37% in patients with the CA or AA allele. On the other hand, the second best predictor for those patients with a baseline Hb concentration above 14 g/dl was the *ITPA* genotype. Patients with the AA or AC allele had the lowest incidence of anemia (17%). For those with the *ITPA* CC allele, CLcr was the third best predictor; the optimal cutoff value was 85 ml/min for this group. The incidence of severe anemia was 49% in patients with a CLcr below 85 ml/min while it was 32% in those with a CLcr above 85 ml/min.

Following this analysis, the patients were divided into six groups, with the incidence of severe anemia ranging from 17% to 76%. Three groups with two predictors, having an incidence of anemia >40%, were defined as the high-risk group and the remainder were defined as the low-risk group. The incidence of severe anemia was higher in the high-risk group than the low-risk group (65% vs. 28%, $P = 0.029$) (Fig. 2). Comparison of the *ITPA* genotype and the predictive model showed that the sensitivity for the prediction of severe anemia was similar (75.9% vs. 76.4%) but the specificity of the predictive model was greater (33.6% vs. 59.3%).

The Risk of Anemia Impacts on Sustained Virological Responses by Patients Who Achieved an Early Virological Response

The impact of *IL28B* genotype, *ITPA* genotype, and risk group of anemia on the rate of sustained virological response was studied at baseline and week 12. At baseline, patients with the TT allele of the *IL28B* gene had a significantly higher rate of sustained virological response than those with the TG or GG allele (43% vs. 10%, $P < 0.0001$), the high-risk group for anemia had a significantly lower rate of sustained virological response than the low-risk group (28% vs. 40%, $P = 0.011$), and the *ITPA* genotype was not associated with a sustained virological response (Fig. 3A–C). At week 4, patients with rapid virological response had a high rate of sustained virological response, irrespective of the *IL28B* genotype (TT vs. TG/GG; 97% vs. 100%, $P = 1.000$), the *ITPA* genotype (CC vs. CA/AA; 95% vs. 100%, $P = 1.000$), and the risk of anemia (high vs. low; 95% vs. 100%, $P = 1.000$). Among the patients who did not achieve a rapid virological response, those with the *IL28B* TT allele had a significantly higher rate of sustained virological response than those with the TG or GG allele (38% vs. 8%, $P < 0.0001$), and the high-risk group for anemia had a significantly lower rate of sustained virological response than the low-risk group (24% vs. 35%, $P = 0.015$). At week 12, in patients who achieved a complete early virological response, the *IL28B* genotype was not associated with a sustained virological response, while the high-risk group for anemia had a

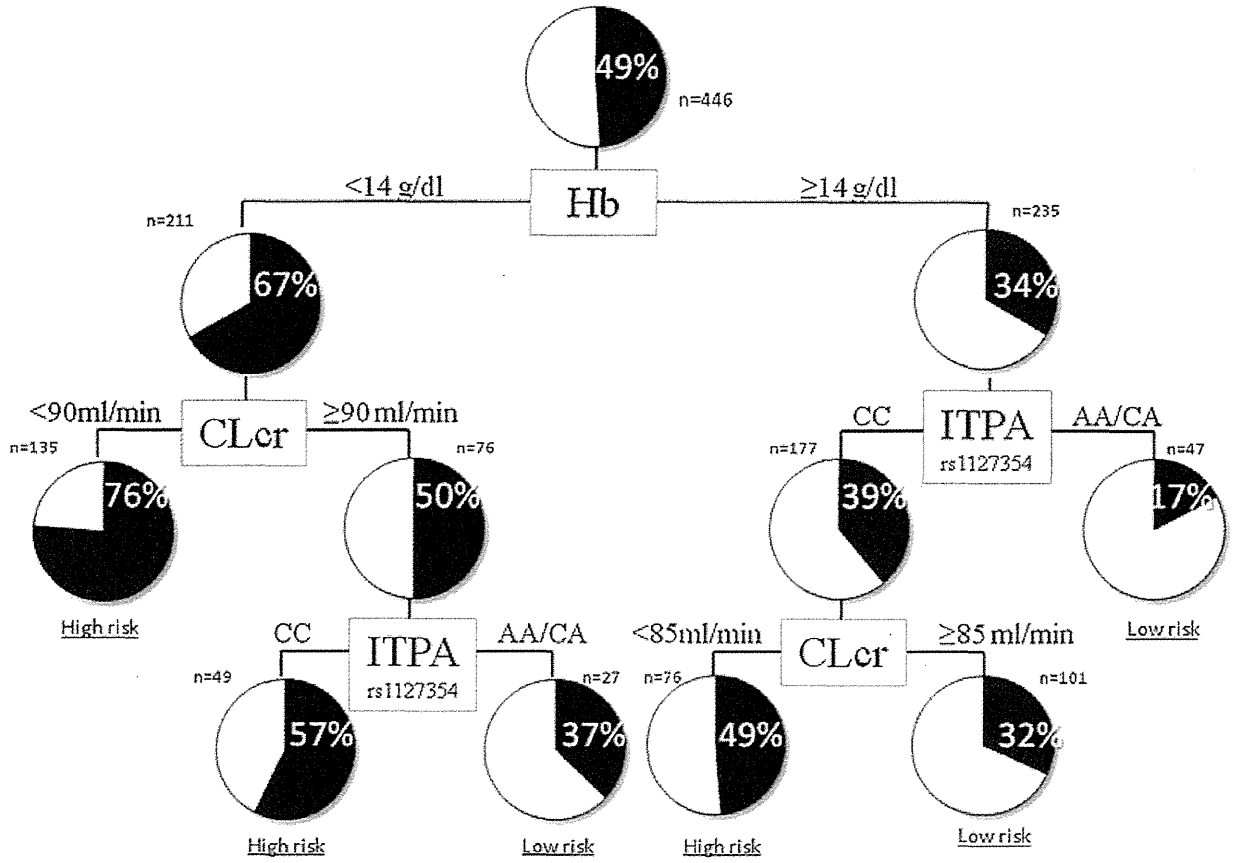

Fig. 1. The predictive model for severe anemia. The boxes indicate the factors used to differentiate patients and the cutoff values for the different groups. The pie charts indicate the rate of severe anemia (Hb <10.0 g/dl) for each group of patients, after differentiation. Terminal groups of patients differentiated by analysis are classified as at high risk if the rate is >40% and low risk if the rate is <40%. *ITPA*, inosine triphosphatase; CLcr, creatinine clearance; Hb, hemoglobin.

significantly lower rate of sustained virological response than the low-risk group (59% vs. 76%, $P = 0.013$) (Fig. 3D–F). In patients who did not achieve a complete early virological response, the *IL28B* genotype was a significant predictor of a sustained virological response (TT vs. TG/GG; 14% vs. 2%, $P < 0.0001$) but a high risk for anemia was not (high vs. low; 10% vs. 6%, $P = 0.361$).

From multivariate analysis (Table II), the *IL28B* genotype was the most important predictor of a sustained virological response at baseline [adjusted odds ratio 9.88 (95% confidence interval 5.01–19.48), $P < 0.0001$], along with female sex [0.42 (0.26–0.68), $P < 0.0001$], platelet count [1.09 (1.04–1.15), $P < 0.0001$], advanced fibrosis [0.49 (0.27–0.91), $P = 0.024$], and baseline HCV RNA load [4.14 (2.27–7.55), $P < 0.0001$]. At week 4, in patients without a rapid virological response, the *IL28B* genotype remained the most important predictor of a sustained virological response [7.16 (3.60–14.25), $P < 0.0001$], along with female sex and platelet count. At week 12, in patients with a complete early virological response, the risk of anemia was an independent and significant predictor of a sustained virological response [0.47 (0.24–0.91), $P = 0.026$], together with the platelet count and HCV RNA load, but the *IL28B* genotype was not associated with a sustained virological response. In patients without a complete early virological response, the *IL28B* genotype was a predictor of a sustained virological response [9.13 (2.02–41.3), $P = 0.004$] along with the platelet count. Thus, *IL28B* was a significant predictor of a sustained virological response at baseline and among virological non-responders at weeks 4 and 12. On the other hand, once a complete early virological response was achieved, the *IL28B* genotype was no longer associated with a sustained virological response but the risk of anemia was an independent predictor of a sustained virological response.

The Risk of Anemia, RBV Dose, and Treatment Outcome in Patients With a Complete Early Virological Response

Patients who achieved a complete early virological response were stratified according to adherence to

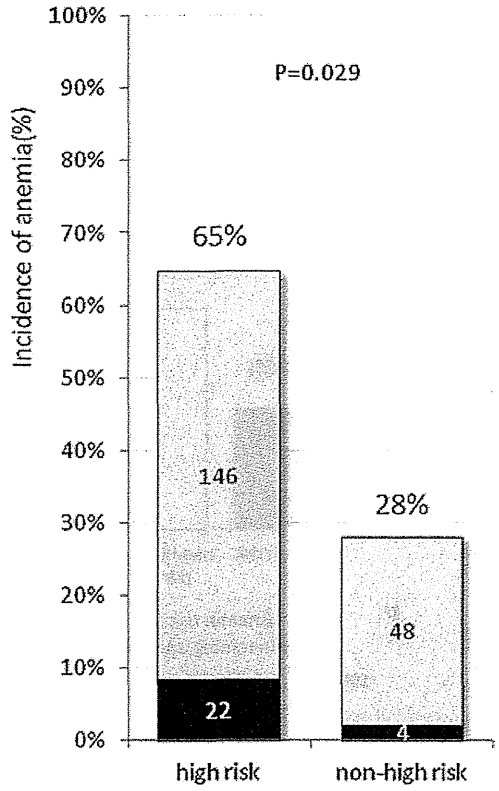

Fig. 2. The incidence of severe anemia stratified by risk of anemia. The incidence of anemia during therapy is shown for each group of patients at high and low risk of anemia. The black and white bars represent the percentages of patients with Hb concentrations below 8.5 g/dl and above 10 g/dl, respectively.

RBV (≤40%, 41–60%, 61–80%, and >80%), which showed that patients with a high risk of anemia were predominantly in subgroups with a lower adherence to RBV (≤40%, 41–60%, and 61–80%), whereas patients with a low risk of anemia were predominantly in subgroups with a higher adherence to RBV (>80%) (Fig. 4, upper panel). The percentage of patients who received >80% of the planned dose of RBV was significantly higher in the low-risk group for anemia than in the high-risk group (74% vs. 55%, $P < 0.0001$).

Within the groups with high and low risks of anemia, there was a stepwise increase in the rate of sustained virological response according to the increase in adherence to RBV (Fig. 4, lower panel). The rate of sustained virological response was higher in patients who received >80% of the planned dose of RBV than those who received less, for both high-risk patients (71% vs. 47%, $P = 0.016$) and low-risk patients (81% vs. 60%, $P = 0.072$). Within the same subgroup of RBV adherence, however, the rate of sustained virological response did not differ between patients with a high risk and a low risk of anemia. Taken together, these results suggest that patients with a high risk of anemia have a disadvantage because they are likely to be intolerant to RBV, leading to reduced adherence to RBV throughout the 48 weeks of therapy and a reduced rate of sustained virological response. However, if >80% adherence to RBV could be obtained, the rate of sustained virological response would increase by 24%.

DISCUSSION

This study confirmed previous reports that the *IL28B* genotype is the most significant predictor of a sustained virological response to PEG-IFN plus RBV therapy in chronic hepatitis C patients at baseline [Ge et al., 2009; Suppiah et al., 2009; Tanaka et al., 2009; Rauch et al., 2010; Kurosaki et al., 2011c] and at week 4 [Thompson et al., 2010b], but it had no impact on the rate of sustained virological response among those patients who achieved a complete early virological response [Thompson et al., 2010b; Kurosaki et al., 2011c]. In contrast, the risk of anemia, assessed by the combination of the *ITPA* genotype, baseline Hb concentration, and baseline CLcr, was found to be associated with a sustained virological response in patients who achieved a complete early virological response. Generally, a complete early virological response is the hallmark of a high probability of a sustained virological response, but the rate of sustained virological responses in patients who achieved a complete early virological response and had a high risk of anemia was as low as 59%. This reduced rate of sustained virological response in these patients was attributable to poor adherence to RBV throughout the 48 weeks of therapy. Because administration of >80% of the planned RBV dose increased the rate of sustained virological response by 24%, it may be postulated that personalizing the treatment schedule to achieve a sufficient dose of RBV, such as extension of treatment duration, may improve sustained virological response rates in these patients. Clearly, this postulate needs to be confirmed in future study. Thus, the findings presented here may have the potential to support selection of the optimum, personalized treatment strategy for an individual patient, based on the risk of anemia.

The degree of hemolytic anemia caused by RBV varies among individuals. A reduction of the Hb concentration early during therapy predicts the likely development of severe anemia [Hiramatsu et al., 2008, 2011] but there are no reliable predictors at baseline. A breakthrough came from the results of a genome-wide association study that revealed that variants of the *ITPA* gene are protective against hemolytic anemia [Fellay et al., 2010]. The *ITPA* genotype has been shown repeatedly to be associated with the degree of hemolytic anemia and dose reduction of RBV [Fellay et al., 2010; Sakamoto et al., 2010; Thompson et al., 2010a; Seto et al., 2011; Tanaka et al., 2011; Kurosaki et al., 2011d]. However, factors other than the *ITPA* gene, such as baseline Hb concentrations [Ochi et al., 2010; Kurosaki et al., 2011d], platelet counts [Ochi

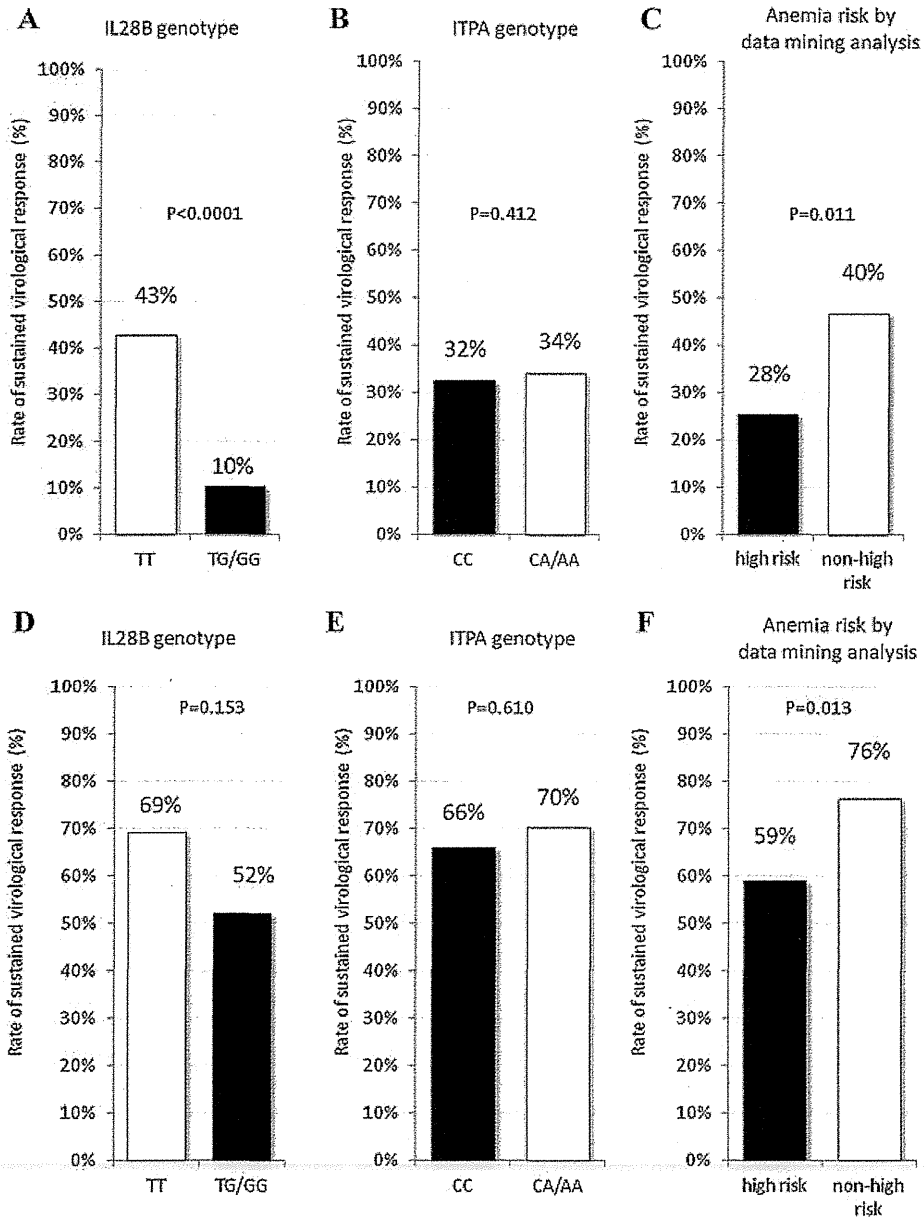

Fig. 3. Rates of sustained virological responses at baseline and among those with a virological response at week 12. The impacts of *IL28B* genotype, *ITPA* genotype, and risk group of anemia on the rate of sustained virological response were studied at baseline (**A–C**) and among those with complete early virological responses (defined as undetectable HCV RNA at week 12) (**D–F**). At baseline, those with the TT allele of the *IL28B* gene had a significantly higher rate of sustained virological response than those with the TG or GG allele and the group at high-risk of anemia had a significantly lower rate of sustained virological response than the low-risk group. Among patients with complete early virological responses, the *IL28B* genotype was not associated with a sustained virological response, while the group at high-risk of anemia had a significantly lower rate of sustained virological response than the low-risk group.

et al., 2010], and CLcr [Kurosaki et al., 2011d], also contribute to the risk of severe anemia or RBV dose reduction. In the present study, the predictive model of anemia based on the data mining analysis selected the *ITPA* genotype, baseline Hb concentration, and baseline CLcr as predictive factors and identified six subgroups of patients with a variable rate of severe anemia, ranging from 17% to 76%. The specificity of the prediction of severe anemia was improved by 25.7% in the predictive model, compared to *ITPA*